PAPER

A mechanistic study on electro-Fenton system cooperating with phangerochate chrysosporium to degrade lignin

Yingjian Qin,[†][a] Na Wang,[†][a] Zhongmin Ma,[a] Jinsheng Li,[b] Yaozong Wang[b] and Lihua Zang 🔾 *[a]

The combined catalytic system of Electro-Fenton (E-Fenton) and *Phanerochaete chrysosporium* (*P. chrysosporium*) was constructed in liquid medium with additional potential to overcome the limitations of lignin degradation by white rot fungi alone. To further understand the mechanism of synergistic catalysis, we optimized the optimum potential for lignin catalysis by *P. chrysosporium* and built synergistic *versus* separate catalyses. After 48 h of incubation, the optimum growth environment and the highest lignin degradation rate (43.8%) of *P. chrysosporium* were achieved when 4 V was applied. After 96 h, the lignin degradation rate of the cocatalytic system was 62% (E-Fenton catalysis alone 22% and *P. chrysosporium* catalysis alone 19%), the pH of the growth maintenance system of *P. chrysosporium* was approximately 3.5, and the lignin peroxidase (LiP) and manganese-dependent peroxidase (MnP) enzyme activities, were significantly better than those of the control. The qPCR results indicated that the expression of both MnP and LiP genes was higher in the cocatalytic system. Meanwhile, FTIR and 2D-HSQC NMR confirmed that the synergistic catalysis was effective in breaking the aromatic functional groups and the side chains of the aliphatic region of lignin. This study showed that the synergistic catalytic process of electro-Fenton and *P. chrysosporium* was highly efficient in the degradation of lignin. In addition, the synergetic system is simple to operate, economical and green, and has good prospects for industrial application.

1. Introduction

Lignocellulose, which is rich in renewable carbon resources, is considered one of the most promising energy alternatives to reduce the overdependence on fossil fuels.[1,2] Unfortunately, the resistance of lignin to filling the cellulose framework to support the cell wall hinders the efficient use of lignocellulose.[3,4] Similarly, black liquor produced in the pulp industry has limited recycling and utilization due to the presence of lignin.[5] Therefore, the degradation of lignin is pivotal for maximizing resource utilization and reducing the environmental pollution burden.[6]

The chemical recalcitrance of lignin stems from its structural complexity.[7] Lignin is an aromatic polymer formed by cross-coupling phenolic units through a variety of ether bonds and carbon–carbon bonds.[8] Among the different methods of lignin degradation, the microbial method has many advantages, such as the conditions are mild and it is simple to operate, with no expensive or designed catalysts, and its

secretion of enzyme catalytic activity and the complex metabolic action degradation of lignin has become an effective natural pathway.[9] Filamentous fungi, especially white rot fungi,[10] have received widespread attention due to their significant effects on wood degradation,[11] papermaking wastewater treatment, and lignocellulose pretreatment.[12] *Phanerochaete chrysosporium* (*P. chrysosporium*) is a typical white rot fungus that penetrates wood cells to produce lignin peroxidase (LiP) and Mn-dependent peroxidase (MnP) to degrade lignin.[13] Between these peroxidases, LiP undergoes a series of oxidations and generates free radicals under the start of hydrogen peroxide (H_2O_2).[14] In most cases, LiP can degrade nonphenolic lignin units by electron transfer *via* an invariant tryptophan residue (trp171), such as C_α–C_β, which breaks the propyl side chain.[7]

In the degradation of lignin, the two peroxidases secreted by *P. chrysosporium* can effectively break the bonds between lignin units and increase the subsequent enzymatic hydrolysis of sugar.[15,16] Unfortunately, LiP and MnP mainly attack the end groups or simple substrates of polymers and form short free radicals, which is due to their limited electron transfer.[7] Therefore, their oxidation of lignin lacks the ability to penetrate the entire lignin structure and provide oxidants over a long time. In effect, ferrous ions in the active centre of peroxidase catalyse H_2O_2 to produce the reactive oxygen species (ROSs, mainly including hydroxyl radicals and superoxide radicals),

[a]*College of Environmental Science and Engineering, Qilu University of Technology (Shandong Academy of Science), Jinan, 250353, Shandong, P.R. China. E-mail: Zlh@qlu.edu.cn; Tel: +86 13325127799*

[b]*Weifang Ensign Industry Co., Ltd, Changle, 262499, Shandong, P.R. China*

† Equal authors contribution.

which can be regarded as the Fenton system.[17] A previous study showed that the natural degradation of lignin by white rot fungi simulated by the Fenton system *in vitro* could accelerate the depolymerization of lignin, and the mechanism of lignin degradation by the Fenton system was preliminarily revealed.[18] It was found that the demethoxylation (Lars Hildén *et al.*, 2000) of lignin was carried out, after which the electron transfer to the side chain results in the rupture of the β-O-4 ether bond.[18] In addition, a previous study showed that the Fenton process combined with bioremediation technology had high efficiency in the degradation of organic polymer compounds in waste-water.[19] However, previous studies, only focused on the application of *P. chrysosporium* or the Fenton process for lignin degradation, and refined in-depth studies on the combination of the two were lacking. Meanwhile, the fact that the addition of H_2O_2 brings economic restrictions to the industrialization of technology cannot be ignored. Subsequently, we learned that the continuous *in situ* generation of H_2O_2 by electro-Fenton (E-Fenton) technology requires only an applied electrical potential under acidic conditions to improve the industrial cost and safety risk limits inherent to the use of additional agents.[20] The stimulation of the applied potential and generation of hydrogen peroxide *in situ* activated LiP and MnP and triggered the enzyme cycle, thereby expediting the degradation of lignin.[21] The above shows that electro-Fenton is superior to conventional Fenton technology in terms of economic costs and practical applications. On the other hand, the acidic conditions of the E-Fenton reaction are provided by the production of small organic acids and fatty acids during the culture and metabolism of *P. chrysosporium*.[22] Therefore, the interesting combined synergistic effect of the E-Fenton process and enzymatic hydrolysis of white rot fungi provides a novel idea for lignin degradation.

The combination of E-Fenton and *P. chrysosporium* has the advantages of simple operation, low cost, mildness and green-ness, therefore, this paper attempts to construct a composite system of the two to degrade lignin and studies the synergistic mechanism. High purity graphite felt was used as the cathode material for the *in situ* generation of H_2O_2 due to its advantages of high conductivity, large specific surface area, corrosion resistance and good biological resistance. The successful construction of the synergistic system is closely dependent on the adjustment of pH in the E-Fenton system by *P. chrysosporium* and the rapid start of LiP and MnP enzymatic hydrolysis with the addition of trace Fe^{2+} and 4 V potential. Thus, the degradation effect due to the synergy of the two systems was studied. Moreover, related characterization methods, such as enzyme gene expression, FTIR and 2D-HSQC NMR, were systematically carried out to analyse the structural changes of lignin and study the codegradation mechanism.

2. Materials and methods

2.1 Strain, medium and inoculation

P. chrysosporium BKMF-1767 (ATCC 20696) was procured from the Global Bioresource Center (ATCC). The strain was stored on potato dextrose agar (PDA) plates at 4 °C.[23]

Test liquid medium: a 250 mL conical flask was filled with 150 mL of culture solution consisting of lignin (dealkaline) (as a carbon source, 0.5 g L^{-1}), NaCl (0.1 g L^{-1}), MgSO$_4$ (0.1 g L^{-1}), KH$_2$PO$_4$ (1 g L^{-1}), CaCl$_2$·6H$_2$O (0.1 g L^{-1}), ammonium tartrate (0.1 g L^{-1}), and trace element solution (3 mL L^{-1}). The trace element solutions included FeSO$_4$·7H$_2$O (1.5 g L^{-1}), CoSO$_4$·7H$_2$O (1 g L^{-1}), ZnSO$_4$·7H$_2$O (1 g L^{-1}), CuSO$_4$·5H$_2$O (20 mg L^{-1}), MnSO$_4$ (0.6 g L^{-1}), and Vitamin B1 (0.6 g L^{-1}). The above reagents were supplied by Sinopharm Chemical Reagent Co., Ltd (Beijing, China).

The PDA slant liquid medium previously stored in the refrigerator at 4 °C was removed, and the mycelium was inoculated into the liquid medium (using glucose as the carbon source) with an inoculation loop, incubated in a shaker at 38 °C for 96 hours and then prepared for use. Mycelium was obtained by filtration using filter paper, washed, weighed and divided equally into subsequent experiments.

2.2 Optimization of catalytic systems

The lignin degradation reactions were carried out in a 250 mL conical flask. A highly stable platinum electrode was used as the anode and a high purity graphite carbon felt made of polyacrylonitrile-based activated carbon fibre was used as the cathode electrode material, maintaining a 10 cm spacing between them.

Determination of optimum potential: The lignin liquid medium inoculated with *P. chrysosporium* was applied with 3 V, 3.5 V, 4 V, 4.5 V, 5 V, and 5.5 V and incubated for 48 h at 60 rpm and 38 °C. Afterwards, the pH, lignin content, and enzymatic activity of the two enzymes were measured by sampling.

2.3 Construction and comparison of the catalytic degradation system of lignin

E-Fenton/enzyme catalysis (E-F/P): *P. chrysosporium* was inoculated into the test liquid medium and then a constant 4 V current was applied. Afterwards, the reaction vessels were placed in a constant temperature shaker with a sterile film seal and incubated for 96 h at 60 rpm and 38 °C. The pH, lignin content, and enzymatic activity of LiP and MnP in the catalytic system were measured every 12 h. Before the experiment, high-temperature autoclave treatment was performed, and the culture unit was assembled on a sterile table.

E-Fenton catalysis (E-F): In this degradation system, no bacteria were inoculated, only the applied potential was provided, and other conditions and assays were consistent with E-F/P.

Enzyme catalysis (P): in this system, only the bacteria were inoculated, no power was applied, and all other conditions and assays were kept consistent with E-F/P.

In addition, a one-way analysis of variance (ANOVA) was performed to examine for significant variations with the statistical function of origin.

2.4 Calculation of lignin degradation rate

The principle was to quantify the change in lignin content by acetylating the phenolic hydroxyl group in lignin with the test

reagent and then measuring its characteristic peak at 280 nm with an enzyme labeller (Tecan Infinite 200Pro).

The lignin degradation ratio was calculated using the following formula:

$$R(\%) = 100 \times (m_0 - m)/m_0$$

where R is the degradation ratio for the sample, m_0 is the initial content of lignin, and m is the sampling content of lignin.

2.5 Measurement of enzyme activity

LiP activity was measured based on an ultraviolet spectrophotometry that monitored the oxidation process of veratryl aldehyde at 310 nm. The reaction was initiated by the addition of H_2O_2 to the standard reaction mixture. The standard reaction mixture consisted of 1.8 mL of sodium tartrate buffer (250 mM, pH 3.0), 0.6 mL of veratryl alcohol (10 mM), 0.03 mL of hydrogen peroxide solution (40 mM), and 0.6 mL of aqueous enzyme extract.[24]

The MnP activity was determined by ultraviolet spectrophotometer at 290 nm to determine the rate of formation of Mn^{3+} (obtained by oxidation of Mn^{2+}). The reaction was initiated by adding 60 mL of H_2O_2 (10 mM) to the reaction mixture. The reaction mixture contained 2.4 mL of sodium succinate (50 mM, pH 4.5) and 0.6 mL of enzyme sample.[25]

2.6 Determination of the relative expression of the Lip and MnP genes

The total RNA of *P. chrysosporium* was extracted from E-Fenton and lignin-induced and lignin-only induced *P. chrysosporium* in a glucose liquid medium by the liquid nitrogen grinding method. Then, the reaction solution was put into the PCR instrument, and the reaction was carried out according to the following reaction procedure: 37 °C for 15 min; 85 °C for 5 s; and 4 °C for holding. After finishing, it was removed and stored at −20 °C. Finally, qRT–PCR was performed on the three sets of samples with a fluorescent quantitative PCR instrument (Roche, LightCycler 480) to determine the mRNA levels of the LiP and MnP genes produced by the three sets of *P. chrysosporium*. The real-time PCR primer pairs for MnP and LiP of *P. chrysosporium* were: F: 5′-ACTAGTATGGCCTTCAAGTCCCTCA-3′, R: 5′-CCATGGTTATG-CAGGGCCGTTGAAC-3′; F: 5′-ACTAGTATGGCCTTCAAG-CAGCTCT-3′, R: 5′-GCGGCCGCAAGCACCCGGAGGCGG-3′.

2.7 Lignin structural analysis

2.7.1 FTIR spectroscopy analysis. A certain amount of culture solution was taken from the initial test liquid medium and the reacted E-F/P system, E-F system and P system and then dried under vacuum at 60 °C for 24 h. The obtained samples containing lignin were subjected to spectral scanning using the KBr press method with a Thermo Scientific Nicolet iS20 infrared spectrometer in the range of 400–4000 cm^{-1} with 32 scans and a resolution of 4 cm^{-1}.

2.7.2 2D-HSQC NMR analysis. Lignin samples were sampled and dried as described in the FTIR spectroscopy analysis, and then four sets of samples were dissolved in

deuterated dimethyl sulfoxide and placed on a Bruker AVAN-CEIIIHD500 NMR spectrometer to measure ^1H and ^{13}C NMR spectra. The 2D-HSQC NMR was resolved using MestReNova 12 and compared with literature to determine the signal attribution.

3. Results and discussion

3.1 Effect of external potential on the catalytic degradation of bacteria

In this study, potential gradients of 3 V, 3.5 V, 4 V, 4.5 V and 5 V were set to determine the optimum potential for *P. chrysosporium* catalysis by electric fields. The pre-experiments showed that the data of the E-Fenton combined with *P. chrysosporium* catalytic system at different potentials were basically stable and that the comparison trend was obvious after 48 h, so 48 h was chosen as the observation time point. Fig. 1 shows that the catalytic effect of *P. chrysosporium* was not proportional to the potential intensity of the electric field with a tendency of promoting and then inhibiting. This was attributed to the activating effect of H_2O_2, which was provided by the E-Fenton system constructed by the applied electric field, on MnP and LiP. However, larger potentials (>4 V) produce more H_2O_2, causing the high concentration of ROSs to exceed the antioxidant capacity of *P. chrysosporium*, resulting in oxidative stress.[26,27] Further, cell membrane rupture or damage to DNA and proteins in *P. chrysosporium* leads to cell death and impaired catalytic lignin breakdown. In agreement with the results of Fig. 1c and d, the inhibition of Lip and Mnp activity occurred at >4 V.[28,29] According to Fig. 1, when the externally applied potential was 4 V, the lignin degradation rate reached 43.8% after 48 h, and the activities of MnP and LiP reached maximum values of 355.1 (U L^{-1}) and 50.15 (U L^{-1}), respectively. This was attributed to the fact that ROSs, which has a high oxidation capacity, was produced by the catalytic decomposition of H_2O_2 generated by E-Fenton in the presence of ferrous ions, which promoted the oxidation of lignin.[30] In addition, within the voltage range tolerated by the bacterium, approximately 4 V optimally increased the permeability of the bacterium's cell membrane, facilitating the transport of nutrients[31] and increasing the stimulation and release of enzymes, thus improving the degradation of lignin. In addition, 4 V promoted the rapid growth of *P. chrysosporium*, causing it to metabolize lignin fragments to secrete organic acids, promoting a rapid decrease in environmental pH and providing the optimum acidic conditions for E-Fenton.[32,33] These results indicated that 4 V was the optimum potential for *P. chrysosporium* to catalyse lignin degradation within a certain potential range.

3.2 Synergistic catalysis for lignin degradation

Based on the above results, the external application of E-Fenton combined with *P. chrysosporium*-catalysed lignin degradation (E-F/P) was set as the experimental group, only potentiometric formation of the E-Fenton system to catalyse lignin degradation (E-F) was set as control Group 1, and only *P. chrysosporium*-
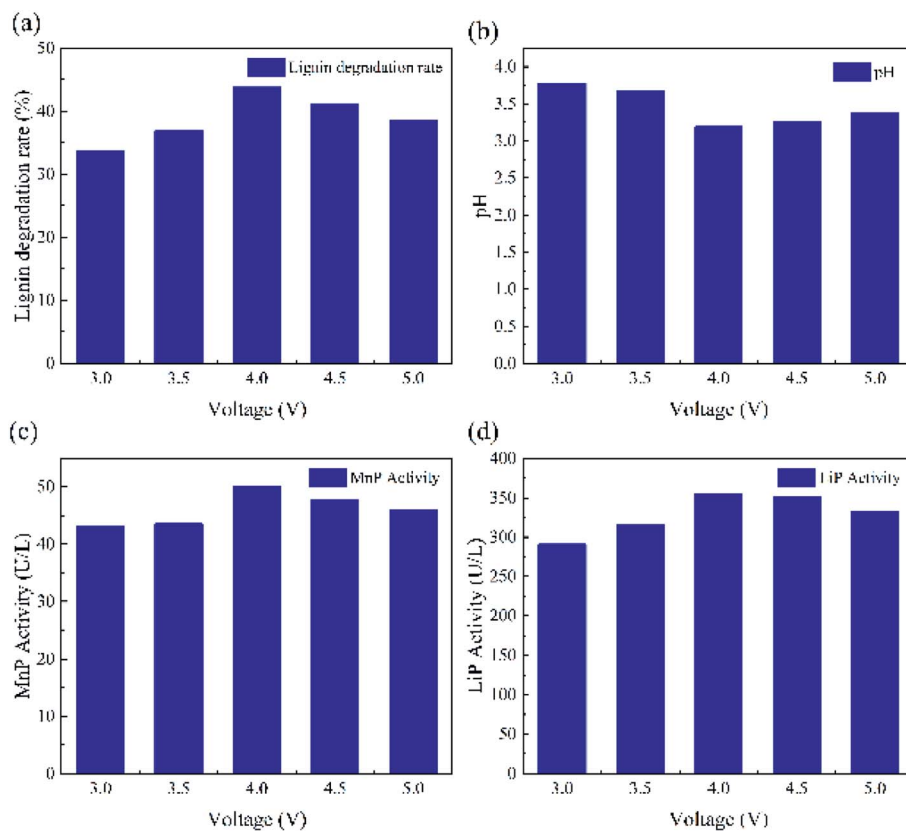
Fig. 1 Degradation rate of lignin (a), pH value (b) and MnP (c) and LiP (d) activity of *P. chrysosporium* cultured for 48 h under different applied potentials.

catalysed lignin degradation (P) was set as control Group 2. After 96 h of incubation, the catalytic degradation rates of the three groups for lignin are shown in Fig. 2(a): E-F/P 62%, E-F 22%, and P 19%. By tracking the lignin degradation effect of each group, it was found that the degradation rate of lignin by E-F/P was greater than that of the control group in all time periods, which indicated that the combined effect of E-Fenton and *P. chrysosporium* greatly promoted the degradation of lignin ($p < 0.05$., indicating that there was a significant difference between the experimental group and the control group). This was related to the strong oxidation of ROSs provided by electro-Fenton to break the lignin functional group.

The pH values of different culture stages are shown in Fig. 2(b). As the incubation progressed, the pH of E-F/P dropped more rapidly and eventually stabilized at a lower value than that in the control group. The pH of E-F/P dropped rapidly from an initial value of 4.7 to approximately 3, and then the pH began to rise slowly and eventually stabilized at approximately 3.5, as a result of the synergistic effect of E-Fenton and *P. chrysosporium*. This was because when the fungal cells were placed in an applied potential of a suitable intensity, the permeability of the cell membrane was improved, which was beneficial to the introduction of various exogenous substances into living cells[34] and accelerated the metabolic activity of *P. chrysosporium*.[28,35–37] Microorganisms convert polysaccharides to organic acids during lignin degradation, which leads to a faster pH drop in E-

F/P. Therefore, the acidic environment created by *P. chrysosporium* became necessary to constitute an E-Fenton. No additional acid was required to adjust the pH making the whole process greener and more economical. In addition, the microorganisms made further use of organic acids, promoting a rise in pH at the end of the culture.

As shown in Fig. 2c and d, E-F/P and P showed similar trends in the enzyme activity tests for LiP or MnP, but the enzyme activities of both enzymes were higher in the E-F/P synergistic system than in the control. The experimental data showed that the changes in the two enzymes could be roughly divided into three stages. With increasing culture time, the changes first decreased, then increased, and gradually began to decline after reaching a certain level. This may be attributed to the period of adaptation shown by *P. chrysosporium* to lignin as a carbon source, a period of growth that occurs with the use of lignin or electrical potential stimulation, and the period of weakening as the degradation and conversion of the carbon source leads to a gradual decrease in *P. chrysosporium* metabolism. The figure demonstrates the ability of E-Fenton to promote the catalytic reaction of enzymes in *P. chrysosporium*, which is consistent with the qPCR results. This was attributed to H_2O_2, which was cathodically generated in E-Fenton (4 V) cocatalysis with *P. chrysosporium* and rapidly initiated the hydrolysis of LiP and MnP to accelerate the process of lignin biodegradation.
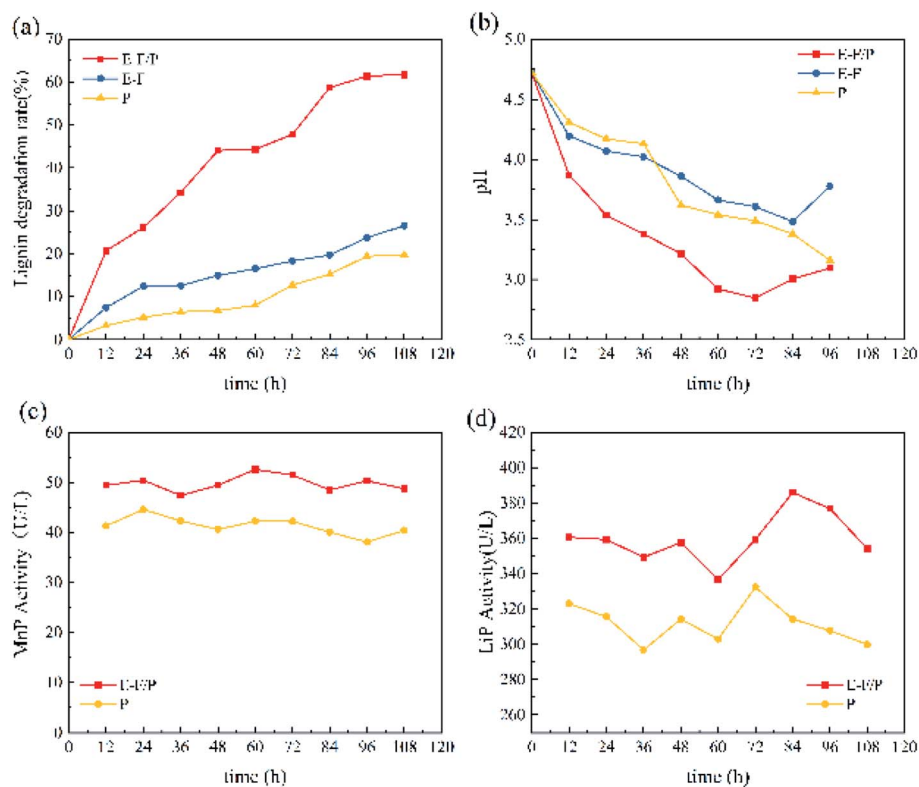
Fig. 2 Degradation rate of lignin (a), pH value (b) and MnP (c) and LiP (d) activity of E-Fenton/enzyme catalysis (E-F/P), E-Fenton catalysis (E-F) and Enzyme catalysis (P) systems.

3.3 Gene expression analysis of LiP and MnP

As shown in Fig. 3, the mRNA levels of *P. chrysosporium* were compared after E-Fenton and lignin induction, and lignin only induction was compared for 48 h. Among them, the utilisation of LiP and MnP played a vital role in the catalytic degradation of lignin. MnP is a peroxidase containing haemoglobin and requires H_2O_2 to initiate the reaction. MnP uses Mn^{2+} as an electron donor, peroxidizing to produce Mn^{3+} and then chelating with dicarboxylic acids to form a stable chelated Mn^{3+}, which acts as a mediator in redox reactions.[38] LiP was also
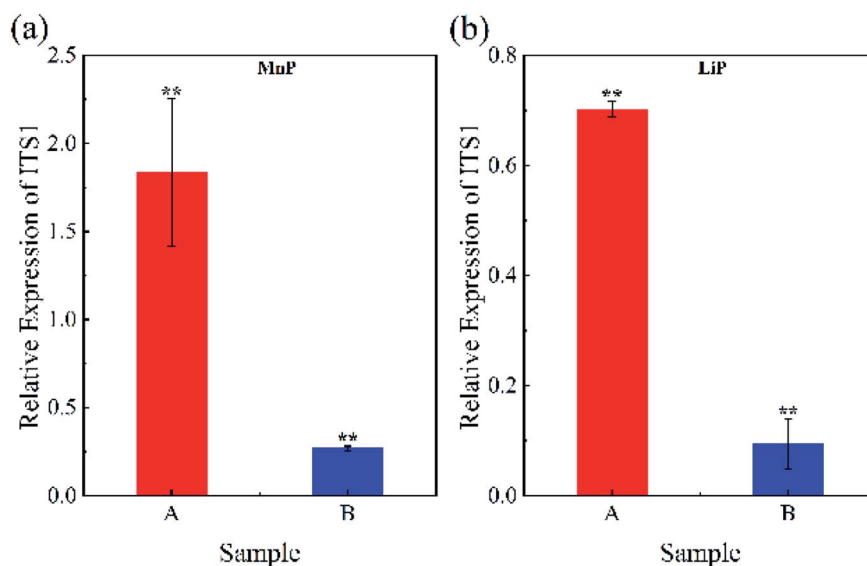

Fig. 3 Gene expression changes in *P. chrysosporium*, where A was the strain coinduced with E-Fenton and lignin, and B was the strain induced with lignin only.

initiated by H_2O_2, which degraded the alkyl side chains of lignin by generating aryl cation radicals for a variety of catalytic oxidation reactions.[39–41] During enzymatic transcription, the gene expression of both MnP and LiP was higher in the E-F/P system than in the P system, which may be induced by the stress response mechanism[42] generated by E-Fenton. In addition, based on the changes in gene expression within the two enzymes in the three groups of samples, it was known that the expression of the MnP gene was higher than that of LiP under potential induction. This indicates that MnP is the main enzyme gene that catalyses the degradation of lignin under this potential condition. Meanwhile, a genetic perspective confirmed that the E-Fenton combined with *P. chrysosporium* catalytic system favours the degradation of lignin.

The above results indicated that there was indeed some synergy of action between E-Fenton and the bacteria to promote lignin degradation. The reasons for the synergistic effect can be summarized as follows: (1) at the appropriate electrical potential, H_2O_2 was rapidly produced by the cathodic oxygen reduction reaction (ORR) and slowly secreted by *P. chrysosporium*, initiating the enzymatic digestion of LiP and MnP.[43] (2) Simultaneously, the appropriate electrical potential increased *P. chrysosporium* cell membrane permeability, accelerating material transport and promoting lignin degradation.[31,34] (3) As *P. chrysosporium* grew at 4 V electrical potential, its secreted organic acids lowered the pH of the environment, and together with Fe^{2+} in the system, the generated H_2O_2 constituted an electro-Fenton reaction, generating ROSs to act indiscriminately on the lignin functional group.[44] (4) Low molecular weight compounds with reducing ability secreted by *P. chrysosporium*, such as organic acids, fatty acids, Fe^{3+} chelators and catechol derivatives, can reduce Fe^{3+} to Fe^{2+} and carry out a cyclic synergistic oxidation of lignin.[45,46] The mechanism is shown in Fig. 4. This synergistic catalytic system provided H_2O_2 and an acidic environment to effectively reduce the cost, while the

enzyme and ROSs cocatalysis enhanced the degradation of lignin, making it an effective strategy for lignin degradation.

3.4 Structural analysis of lignin

The alteration of the structure of untreated lignin and three groups of treated lignin was investigated by FTIR. As shown in Fig. 5, the O–H stretching originating from both aromatic and aliphatic groups can be clearly observed at approximately $3270\ cm^{-1}$. However, the centres of their absorption peaks were clearly different, and all three treatment groups showed varying degrees of redshift here relative to the original lignin sample ($3284.56\ cm^{-1}$). It was possible that the hydrogen bond formed during the catalysis process weakened the O–H bond stretching vibration, and at the same time, there may also be a conjugated system formed after the reaction that caused the peak to shift to a low wavenumber.[47] Among them, the strongest redshift ($3199.13\ cm^{-1}$) was observed after the E-F/P synergistic treatment. The characteristic signals at 2925 and $2854\ cm^{-1}$ were attributed to methylene groups in the lignin side chain structure,[48] and for the three sets of experiments, only the lignin
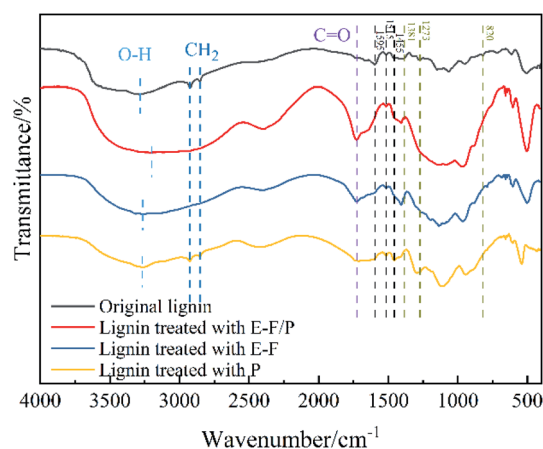

Fig. 5 FTIR spectra of original lignin and lignin treated with E-F/P, E-F and P.
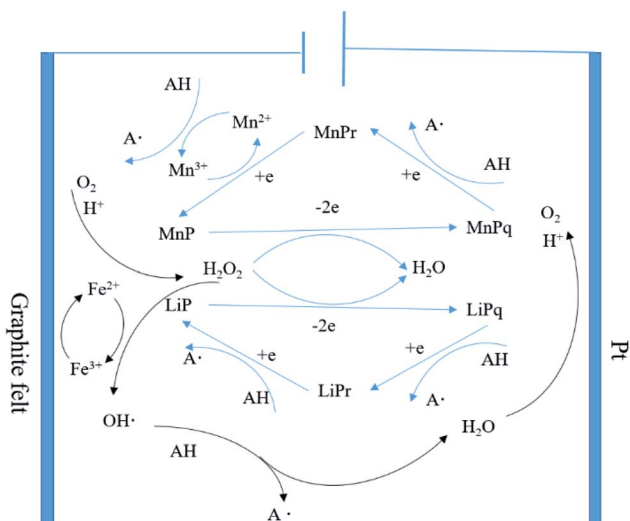

Fig. 4 Proposed mechanism of the synergistic degradation of lignin by the E-Fenton reaction and *P. chrysosporium*.
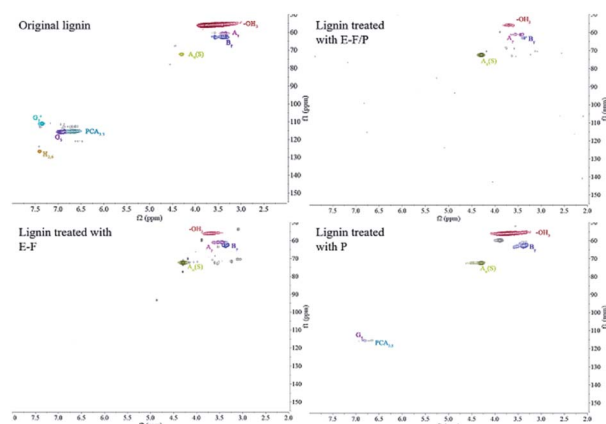

Fig. 6 2D-HSQC NMR spectra of original lignin and lignin treated with E-F/P, E-F and P.

© 2022 The Author(s). Published by the Royal Society of Chemistry

Table 1 Assignments of $^{13}C-^{1}H$ cross-peaks in HSQC spectra of the lignin fractions

Label	δ_C/δ_H (ppm)				Assignment
	Original lignin	Lignin treated with E-F/P	Lignin treated with E-F	Lignin treated with P	
$-OCH_3$	55.79/3.33–3.78	55.79/3.70	55.79/3.68	55.79/3.72	C–H in methoxyls
A_γ	60.96/3.38	60.96/3.45	60.96/3.44		$C_\gamma-H_\gamma$ in γ-hydroxylated β-O-4' substructures (A)
B_γ	62.25/3.33	62.89/3.36	62.89/3.37	62.57/3.38	$C_\gamma-H_\gamma$ in phenylcoumaran substructures (B)
$A_\alpha(S)$	72.26/4.30	72.28/4.28	72.26/4.30		$C_\alpha-H_\alpha$ in β-O-4' substructures (A) linked to a S-unit
G_2'	111.00/7.35				C_2-H_2 in oxidized guaiacyl units (G')
PCA$_{3,5}$	115.52/6.66			115.19/6.66	C_3-H_3 and C_5-H_5 in p-coumarate (PCA)
G_5	115.85/6.96			115.52/6.87	C_5-H_5 in guaiacyl units (G)
$H_{2,6}$	126.49/7.41				$C_{2,6}-H_{2,6}$ in p-hydroxyphenyl units (H)

retained the side chain after enzyme treatment. This indicated that *P. chrysosporium* treatment alone was very mild, while the externally applied potential helped to improve the catalytic effect. More importantly, the characteristic signal of the carbonyl group was significantly enhanced by the E-F/P treatment compared to the P and E-F treatments (approximately 1725 cm^{-1}).

The aromatic skeleton of lignin corresponds to approximately 1595 cm^{-1}, 1515 cm^{-1} and 1455 cm^{-1}. After P treatment alone, the characteristic signal did not change significantly, but the characteristic signal overlapped or disappeared when the potential was given, especially when the enzyme was combined with E-Fenton, indicating that electricity plays an important role in the induction of catalysis of the enzyme. The characteristic signals at approximately 1381 cm^{-1}, 1273 cm^{-1} and 820 cm^{-1} corresponded to guaiacyl (G), syringyl (S) and p-hydroxyphenyl (H) in the lignin structure, respectively, which clearly showed that the three catalytic groups had certain degradation effects on the lignin monomer.[49] In summary, the FTIR results showed that the magnitude of the effect of the three catalytic systems on the lignin structure occurs in the following order: E-F/P > F > P, and that the combined treatment of E-Fenton and enzyme has a synergistic catalytic effect. The structure and composition of untreated-lignin and three groups of treated lignin were resolved by 2D-HSQC NMR. The 2D-HSQC spectra of lignin are shown in Fig. 6 and attributed according to the published literature,[49–51] and its corresponding signal attribution can be found in Table 1. The overall analysis of Fig. 6 shows that after the three catalysts, the signal intensity of the side chain structure in the aliphatic region (δ_C/δ_H 50–90/2.5–5.8) was correspondingly weakened and the signal of the functional group in the lignin aromatic region (δ_C/δ_H 90–150/5.5–8.5) almost disappeared. Fig. 6 shows that the intensity of the C–H signal of the methoxyl group, one of the characteristic functional groups of lignin, was as follows in the spectrum of the three groups of catalysed lignin: Origin > P > E-F > E-F/P. Therefore, E-Fenton and *P. chrysosporium* played a synergistic catalytic role in the degradation of methoxyl. B_γ was

consistent with the methoxyl change in catalysis. In addition, β-O-4 was the main bonding signal of the lignin side chain structure,[52] and A_γ was more favourably degraded in the E-F/P treatment, but the $A_\alpha(S)$ intensity was enhanced with the degradation of lignin. Moreover, the G_2', PCA$_{3,5}$, G_5 and $H_{2,6}$ found in the initial lignin spectra all disappeared almost completely in the E-F and E-F/P treatments, indicating that the electrocatalysis seen here was more complete than that of pure bacteria. In conclusion, the synergistic degradation effect on lignin was exerted by the catalytic system of E-Fenton combined with *P. chrysosporium*, which was consistent with the FTIR results of lignin before and after the three sets of catalytic treatments.

4. Conclusions

The catalytic system of E-Fenton combined with *P. chrysosporium* synergistically promoted the degradation of lignin. Among them, 4 V became the optimum potential to promote the growth and codegradation of lignin by *P. chrysosporium*. In a control experiment with 96 h of lignin degradation, the lignin degradation rate (62%) and the enzymatic activities of MnP and LiP were significantly higher in E-F/P than in E-F and P, which had the lowest acidity. There was an increase in the gene expression of both MnP and LiP after the application of a suitable electrical potential. In the synergistic system, aliphatic side chains such as aromatic framework β-O-4 and the corresponding functional groups of lignin were completely broken. In summary, E-Fenton and *P. chrysosporium* were mutually reinforcing, were closely mutually beneficial and had significant advantages in the catalytic degradation of lignin.

Author contributions

Yingjian Qin: visualization, writing – original draft, data curation. Na Wang: visualization, writing – original draft, data curation. Zhongmin Ma: data curation, investigation. Jinsheng Li: investigation. Yaozong Wang: investigation. Lihua Zang: conceptualization, writing – review & editing.

Conflicts of interest

Acknowledgements

References

1 D. M. Kato, N. Elia, M. Flythe and B. C. Lynn, *Bioresour. Technol.*, 2014, **162**, 273–278.

2 R. Zhou, R. Zhou, S. Wang, U. G. Mihiri Ekanayake, Z. Fang, P. J. Cullen, K. Bazaka and K. K. Ostrikov, *Bioresour. Technol.*, 2020, **318**, 123917.

3 C. Xu, J. Zhang, Y. Zhang, Y. Guo, H. Xu, C. Liang, Z. Wang and J. Xu, *Int. J. Biol. Macromol.*, 2019, **141**, 484–492.

4 W. Zhang, W. Wang, J. Wang, G. Shen, Y. Yuan, L. Yan, H. Tang and W. Wang, *Appl. Environ. Microbiol.*, 2021, **87**, e01321–e01355.

5 S. Zhang, J. Xiao, G. Wang and G. Chen, *Bioresour. Technol.*, 2020, **304**, 122975.

6 E. Subbotina, T. Rukkijakan, M. D. Marquez-Medina, X. Yu, M. Johnsson and J. S. M. Samec, *Nat. Chem.*, 2021, **13**, 1118–1125.

7 K. E. Hammel and D. Cullen, *Curr. Opin. Plant Biol.*, 2008, **11**, 349–355.

8 X. Shen, Y. Xin, H. Liu and B. Han, *ChemSusChem*, 2020, **13**, 4367–4381.

9 C. Cai, Z. Xu, H. Zhou, S. Chen and M. Jin, *Sci. Adv.*, 2021, **7**, eabg4585.

10 M. Asgher, A. Wahab, M. Bilal and H. M. Nasir Iqbal, *Biocatal. Agric. Biotechnol.*, 2016, **6**, 195–201.

11 E. Bari, K. Ohno, N. Yilgor, A. P. Singh, J. J. Morrell, A. Pizzi, M. A. Tajick Ghanbary and J. Ribera, *Microorganisms*, 2021, **9**, 247.

12 X. Qin, X. Su, H. Luo, R. Ma, B. Yao and F. Ma, *Biotechnol. Biofuels*, 2018, **11**, 58.

13 L. Jin, G. Zeng, H. Chen, L. Wang, H. Ji, S. Lin, R. Peng and D. Sun, *BioResources*, 2021, **16**, 5494–5507.

14 L. Thanh Mai Pham, M. H. Eom and Y. H. Kim, *Enzyme Microb. Technol.*, 2014, **61–62**, 48–54.

15 R. Potumarthi, R. R. Baadhe, P. Nayak and A. Jetty, *Bioresour. Technol.*, 2013, **128**, 113–117.

16 F. Q. Wang, H. Xie, W. Chen, E. T. Wang, F. G. Du and A. D. Song, *Bioresour. Technol.*, 2013, **144**, 572–578.

17 R. D. Villa, A. G. Trovo and R. F. Nogueira, *Chemosphere*, 2008, **71**, 43–50.

18 J. Zeng, C. G. Yoo, F. Wang, X. Pan, W. Vermerris and Z. Tong, *ChemSusChem*, 2015, **8**, 861–871.

19 C. Hu, D. Huang, G. Zeng, M. Cheng, X. Gong, R. Wang, W. Xue, Z. Hu and Y. Liu, *Chem. Eng. J.*, 2018, **338**, 432–439.

20 C.-H. Feng, F.-B. Li, H.-J. Mai and X.-Z. Li, *Environ. Sci. Technol.*, 2010, **44**, 1875–1880.

21 C. Yang, S. Maldonado and C. R. J. Stephenson, *ACS Catal.*, 2021, **11**, 10104–10114.

22 V. Arantes, A. M. Milagres, T. R. Filley and B. Goodell, *J. Ind. Microbiol. Biotechnol.*, 2011, **38**, 541–555.

23 F. C. Michel, E. A. Grulke and C. A. Reddy, *J. Ind. Microbiol.*, 1990, **5**, 103–112.

24 H. Tanaka, K. Koike, S. Itakura and A. Enoki, *Enzyme Microb. Technol.*, 2009, **45**, 384–390.

25 X. Peng, X.-z. Yuan, G.-m. Zeng, H.-j. Huang, H. Wang, H. Liu, S. Bao, Y.-j. Ma, K.-l. Cui, L.-j. Leng and Z.-h. Xiao, *Sep. Purif. Technol.*, 2014, **123**, 164–170.

26 M. Jaszek, J. Żuchowski, E. Dajczak, K. Cimek, M. Grąz and K. Grzywnowicz, *Int. Biodeterior. Biodegrad.*, 2006, **58**, 168–175.

27 D. J. Jamieson, *Redox Rep.*, 1995, **1**, 89–95.

28 L. Loghavi, S. K. Sastry and A. E. Yousef, *Biotechnol. Bioeng.*, 2007, **98**, 872–881.

29 B. Ezraty, A. Gennaris, F. Barras and J. F. Collet, *Nat. Rev. Microbiol.*, 2017, **15**, 385–396.

30 M. A. Fernandez de Dios, A. G. del Campo, F. J. Fernandez, M. Rodrigo, M. Pazos and M. A. Sanroman, *Bioresour. Technol.*, 2013, **148**, 39–46.

31 L. Hou, D. Ji, W. Dong, L. Yuan, F. Zhang, Y. Li and L. Zang, *Front. Bioeng. Biotechnol.*, 2020, **8**, 99.

32 J. Jellison, J. Connolly, B. Goodell, B. Doyle, B. Illman, F. Fekete and A. Ostrofsky, *Int. Biodeterior. Biodegrad.*, 1997, **39**, 165–179.

33 M. Humar, M. Petrič and F. Pohleven, *Eur. J. Wood Wood Prod.*, 2001, **59**, 288–293.

34 A. Garg, I. M. Mishra and S. Chand, *Clean: Soil, Air, Water*, 2010, **38**, 27–34.

35 J. Cameron Thrash and J. D. Coates, *Environ. Sci. Technol.*, 2008, **42**, 3921–3931.

36 A. Schievano, T. Pepe Sciarria, K. Vanbroekhoven, H. De Wever, S. Puig, S. J. Andersen, K. Rabaey and D. Pant, *Trends Biotechnol.*, 2016, **34**, 866–878.

37 N. Matsumoto, S. Nakasono, N. Ohmura and H. Saiki, *Biotechnol. Bioeng.*, 1999, **64**, 716–721.

38 G.-M. Zeng, M.-H. Zhao, D.-L. Huang, C. Lai, C. Huang, Z. Wei, P. Xu, N.-J. Li, C. Zhang, F.-L. Li and M. Cheng, *Int. Biodeterior. Biodegrad.*, 2013, **85**, 166–172.

39 O. D. V. Biko, M. Viljoen-Bloom and W. H. van Zyl, *Enzyme Microb. Technol.*, 2020, **141**, 109669.

40 G. Janusz, K. H. Kucharzyk, A. Pawlik, M. Staszczak and A. J. Paszczynski, *Enzyme Microb. Technol.*, 2013, **52**, 1–12.

41 D. W. Wong, *Appl. Biochem. Biotechnol.*, 2009, **157**, 174–209.

42 N. Garcia-Ortiz, F. J. Figueroa-Martinez, U. Carrasco-Navarro, E. Favela-Torres and O. Loera, *Fungal Biol.*, 2018, **122**, 487–496.

43 J. A. Mir-Tutusaus, R. Baccar, G. Caminal and M. Sarra, *Water Res.*, 2018, **138**, 137–151.

44 F. Li, H. Zhao, R. Shao, X. Zhang and H. Yu, *J. Agric. Food Chem.*, 2021, **69**, 7104–7114.

45 V. Arantes and A. M. F. Milagres, *Process Biochem.*, 2006, **41**, 887–891.

46 A. Gutierrez, J. C. del Rio, M. J. Martinez-Inigo, M. J. Martinez and A. T. Martinez, *Appl. Environ. Microbiol.*, 2002, **68**, 1344–1350.

47 M. Lei, S. Wu, C. Liu, J. Liang and R. Xiao, *Fuel Process. Technol.*, 2021, **217**, 106812.

48 A. Tejado, C. Pena, J. Labidi, J. M. Echeverria and I. Mondragon, *Bioresour. Technol.*, 2007, **98**, 1655–1663.

49 Y.-h. Ci, F. Yu, C.-x. Zhou, H.-e. Mo, Z.-y. Li, Y.-q. Ma and L.-h. Zang, *Green Chem.*, 2020, **22**, 8713–8720.

50 J. C. del Rio, J. Rencoret, P. Prinsen, A. T. Martinez, J. Ralph and A. Gutierrez, *J. Agric. Food Chem.*, 2012, **60**, 5922–5935.

51 H. Kim, J. Ralph and T. Akiyama, *BioEnergy Res.*, 2008, **1**, 56–66.

52 B. Wang, X.-J. Shen, J.-L. Wen and R.-C. Sun, *RSC Adv.*, 2016, **6**, 57986–57995.